Conference Proceedings

EuroSun 2014
Aix-les-Bains (France), 16 - 19 September 2014

New Control Strategy for Solar Thermal Systems with several Heat Sinks

Jens Glembin[1], Christoph Büttner[2], Jan Steinweg[2], Gunter Rockendorf[2] and André Klingenschmidt[3]

[1,2] Institut für Solarenergieforschung Hameln/Emmerthal (ISFH), Am Ohrberg 1, 31860 Emmerthal, Germany

[1] Phone: +49 5151/999-647, Mail: glembin@isfh.de

[3] RESOL Elektronische Regelungen GmbH, Heiskampstraße 10, 45527 Hattingen, Germany, Phone: +49 2324/9648-0

Abstract

Most solar thermal systems have only one heat sink, usually a storage tank. In most cases such systems are equipped with a controller, which compares the current collector temperature with a sensor representing the heat sink conditions, e.g. a temperature sensor in the lower part of the storage tank. However, solar thermal systems may have more than one heat sink to use the solar heat on different temperature levels, thus increasing the solar benefit. The control of such a system needs to permanently determine an independent demand signal for the different heat sinks.

The paper introduces control variants for a solar thermal system operating on different heat sinks. A more theoretical control approach uses the ambient and operating conditions to determine the potential collector temperatures of each heat sink. In a second approach, the collector pump of one defined heat sink is switched on periodically to get the current collector status. The controller uses this information to determine the potential temperatures for all other heat sinks. A detailed simulation study shows that the second, less complex and lower-priced variant leads to a slightly lower system performance than the theoretic approach which can be defined as the benchmark.

Apart from the collector temperature the control has to decide which heat sink should be used in case of more than one positive demand signal. Simulations show that the best results occur if this decision is based on the potential thermal power, taking into account an optimized predefined weighting factor.

1. Introduction

In most applications, solar thermal systems consist of a collector field delivering the solar heat to one heat sink, usually a storage tank. For such systems a simple on/off controller is still state of the art (Kalogirou, 2009).

Fig. 1 shows the principle of a solar thermal system, which is alternatively working on three heat sinks on different temperature levels. Here, a differential controller cannot be used, since the controller has to

- determine a demand signal independently for all heat sinks,
- decide which heat sink should be charged, if more than one demand signal results,
- if already in operation, decide, if the collector is able to charge another heat sink on a differing temperature level.

© 2015. The Authors. Published by International Solar Energy Society
Selection and/or peer review under responsibility of EuroSun2014 Scientific Committee
doi:10.18086/eurosun.2014.03.09 Available at http://proceedings.ises.org

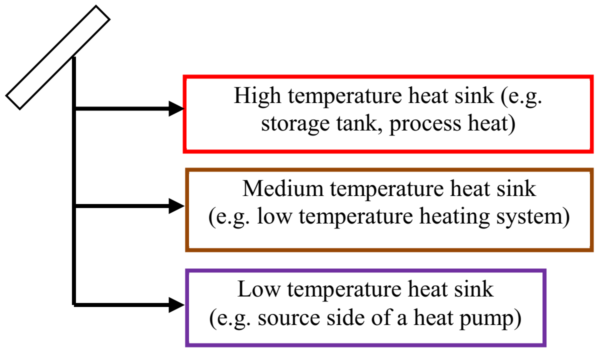

Fig. 1: Scheme of a solar thermal system with three heat sinks on different temperature levels

The paper introduces and analyses two options to control a solar thermal system with several heat sinks which are explained in Section 2. The aim of the investigation is to find the optimum control parameters and particularly the discrepancies between both variants. The evaluation bases on simulations of a complex solar thermal system with three heat sinks in TRNSYS (Klein et al., 2009). Section 3 gives a brief description of this system – a solar active house which is a building with a solar fraction of more than 50%. Within the simulations the main control parameters are varied giving the results presented in Section 4 and discussed in Section 5.

2. Control strategies

As stated in Section 1 it is not possible to control a system with several heat sinks with a simple measurement of the current collector outlet temperature. During operation this single temperature signal does not contain enough information to decide whether a heat sink on a higher temperature level may be charged or not.

An ideal solution is, if the controller knows the potential collector conditions for all heat sinks in advance, i.e. the conditions that would occur if the collector would charge the respective heat sink. This can be realized by implementing collector models in the control algorithm to calculate the collector outlet temperatures based on the ambient and operating conditions of each heat sink. This approach requires additional sensors (e.g. radiation, ambient temperature) and specific parameters (e.g. several collector parameters, aperture area). Thus, it represents a more theoretical method, which will be used as an idealized benchmark. The method is described in Section 2.1 and called idealized control strategy (short: Id-Ctrl).

A more practicable solution was developed based upon the RESOL FlowCon Sensor technology described in Pärisch et al. (2009). In defined time intervals the collector is switched on and charges one defined heat sink. Based on the measured collector outlet temperature operating on this heat sink, the control determines the potential temperatures for all other heat sinks. Compared to the first approach this solution is less complex and requires only a few sensors. As a disadvantage, especially during fast changing conditions, this control may not generate the highest possible collector yield. Moreover, the frequent operation of the collector pump may increase the electricity consumption. This solution is called practical control strategy (short Prac-Ctrl) and described in Section 2.2.

Besides the determination of the demand signals the control needs a decision criterion which heat sink should be used if more than one demand signal occurs. This criterion may be based on the heat sink temperature levels with a clear priority e.g. to charge always on the highest possible temperature level. However, a more complex criterion was developed considering the potential collector yield for each heat sink. These potential yield values may be weighted with an effectivity factor to reach the main goal – the lowest overall energy demand. The method is described more in detail in Section 2.1 but both control strategies may include this weighting factor.

2.1 Idealized control strategy (Id-Ctrl)

The Id-Ctrl calculates several collector outlet temperatures (one for each heat sink) with additional virtual collector circuits. Each circuit represents the subsystem between the collector and the respective heat sink including collector, pipes, valves and heat exchangers. The input temperature to the subsystem is taken from the actual heat sink while the mass flow is always on its heat sink specific nominal value. Each of these control loops represents the operating conditions, if the collector would charge the particular heat sink and the related potential collector outlet temperature is calculated. By comparison of potential collector outlet temperature and heat sink temperature (e.g. temperature in the storage tank) the control is able to decide if charging the respective heat sink is possible.

In case of more than one positive demand signal the controller has to decide which heat sink will be used. A constant priority defines a heat sink, which is always charged at first. Alternatively, the decision may base on the potential collector output power calculated with the potential collector outlet temperatures. Two heat sinks can be compared to each other by the ratio of both output values, defined as W.

$$\left.\begin{aligned}\dot{Q}_{Coll\rightarrow Sink1} &= \dot{m}_{Coll,Sink1}\cdot c_p\cdot(\vartheta_{Coll,out\rightarrow Sink1}-\vartheta_{Sink1})\\ \dot{Q}_{Coll\rightarrow Sink2} &= \dot{m}_{Coll,Sink2}\cdot c_p\cdot(\vartheta_{Coll,out\rightarrow Sink2}-\vartheta_{Sink2})\end{aligned}\right\} W=\frac{\dot{Q}_{Coll\rightarrow Sink1}}{\dot{Q}_{Coll\rightarrow Sink2}} \quad \text{(eq. 1)}$$

The collector charges heat sink 1 ($Sig_{Sink\ 1,t} = 1$) if this ratio is above a defined limit under consideration of an upper and lower controller hysteresis.

$$SIG_{Sink1,t}=1\ \ if\ \begin{cases}SIG_{Sink1,t-1}=0\ and\ W>W_{Set}+\Delta W_{up}\\ SIG_{Sink1,t-1}=1\ and\ W>W_{Set}-\Delta W_{lo}\end{cases} \quad \text{(eq. 2)}$$

W_{Set}-values below 1 indicate a higher priority for heat sink 1 while values above 1 result in a higher priority for heat sink 2. The optimal values of W_{Set} (with the lowest energy demand of the whole system) and its control hysteresis depend on the system design and can be determined with simulations (see Section 4.3). More than one value of W may be used if the system consists of more than two heat sinks. In addition, W may be variable, e.g. it may be a function of the state of the system or a function of the season.

2.2 Practical control strategy (Prac-Ctrl)

The most complicated part of the Id-Ctrl is the determination of the potential collector outlet temperatures which requires additional sensors leading to high costs and additional parameters increasing the risk of failures. The Prac-Ctrl was developed to overcome these disadvantages. The main idea is a regular operation of the collector (within a bypass or a part of a heat sink, e.g. the primary side of a heat exchanger) in defined intervals to measure the actual temperature increase in the collector field.

$$\Delta\vartheta_{Coll,Purge}=\left(\vartheta_{Coll,out,Purge}-\vartheta_{Coll,in,Purge}\right) \quad \text{(eq. 3)}$$

The temperature increase allows the calculation of the potential temperature of each heat sink considering the ratio of mass flow and collector efficiency during purging and while charging the respective heat sink

$$\vartheta_{Coll,out\rightarrow Sink}=\vartheta_{Sink}+\Delta\vartheta_{Coll,Purge}\cdot\frac{\dot{m}_{Coll,Purge}}{\dot{m}_{Coll,Sink}}\cdot\frac{\eta_{Coll,Sink}}{\eta_{Coll,Purge}} \quad \text{(eq. 4)}$$

The efficiency during purging is calculated using the collector efficiency parameters and the measured collector temperatures assuming a constant solar radiation level. The efficiency during charging the heat sink ($\eta_{Coll\rightarrow Sink}$) is calculated in the same manner using the mean collector temperature while in operation based on the measured heat sink temperature ϑ_{Sink} (as the collector inlet temperature) and the requested potential collector outlet temperature $\vartheta_{Coll,out\rightarrow Sink}$. Therefore, the control uses an iterative method to identify collector outlet temperature and efficiency.

After determining all potential collector outlet temperatures the control proceeds in the same way as described for the Id-Ctrl in Section 2.1 including the calculation of potential collector output powers and the value W.

3. Conditions of the system simulations

For a detailed analysis the control variants are investigated within simulations of a new solar active house concept. The collector field delivers heat to three different heat sinks – a buffer storage, a directly heated thermally activated concrete floor (TABS = thermally activated building systems) and a ground heat exchanger, which serves as the heat source for the heat pump representing the back-up heater. The scheme in Fig. 2 gives an overview of the system concept with its main components. A detailed system description is published in Glembin et al. (2014).

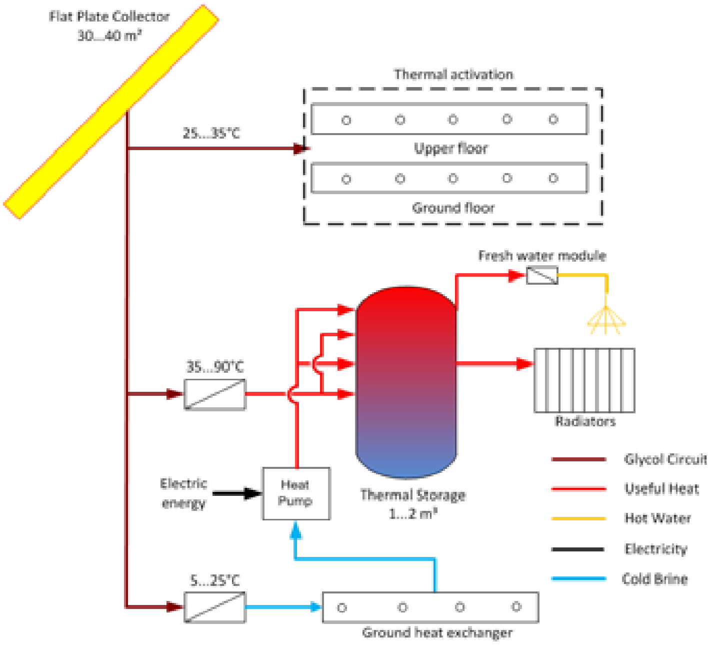

Fig. 2: Scheme of heat sources and heat sinks in the new heating concept for solar houses (the lines indicate energy flows)

The thermal behavior of the concept is calculated in TRNSYS using different control strategies. Apart from the control strategy and its parameters all variants are simulated with the same boundary conditions. The building is parameterized according to the intended design of an exemplarily solar house planned by HELMA Eigenheimbau AG – the overall heat demand is around 10 MWh/a. For more simulation details concerning models and dimensions refer to Glembin et al. (2014).

Both control strategies described in Section 2 are included in the TRNSYS deck. For the Id-Ctrl, a complex control subsystem has been developed including three additional collector subsystems representing the circuits between solar collector and each heat sink. For the Prac-Ctrl a control algorithm developed for a micro controller by RESOL was transferred to the TRNSYS interface and implemented in a new TRNSYS type. This type contains the original source code and determines all control decisions based on the input values (collector and heat sink temperatures). The purging, according to section 2.2, takes place between solar thermal collector and the heat exchanger of the ground circuit.

The ground heat exchanger represents the heat sink with the lowest temperature level where the solar heat is used indirectly to support the heat pumps ground source. Therefore, it has the lowest priority and is only used if both the storage tank and TABS have no demand. A varying priority is used between TABS and storage tank. The controller calculates the potential collector output values according to Section 2.1 and determines the control signal considering the parameter W_{Set}, which will be varied in the simulations (see Section 4.3).

Compared to the Id-Ctrl the Prac-Ctrl requires as additional parameters mainly the duration of the purging interval and the break period between two purging intervals. Both values are varied in simulations to find the optimum variant with the lowest energy demand of the whole system. Table 1 gives an overview of all varied parameters including their values in the base case as well as the minimum and maximum in the variations.

Tab. 1: Varied control parameters

Parameter	Base case value	Minimum value	Maximum value
Purging time interval	90 s	30 s	900 s / 15 min
Purging break interval	30 min	5 min	120 min / 2 h
W_{Set}	1	0	100

4. Results

The main difference between both control variants is the purging process which is analyzed in Section 4.1. The optimum values for the purging parameters are investigated in Section 4.2.

Both control strategies use a variable priority between TABS and buffer storage. Section 4.3 analyses exemplarily for the Prac-Ctrl the system results with different values for W_{Set}.

4.1 Purge interval in detail

In this section, the purge interval of the Prac-Ctrl is analyzed more in detail. Figure 3 gives the temperatures used by the controller to decide about the operation of TABS – the (real) collector in- and outlet temperature, the temperature of the TABS and the potential collector outlet temperature calculated by the control.

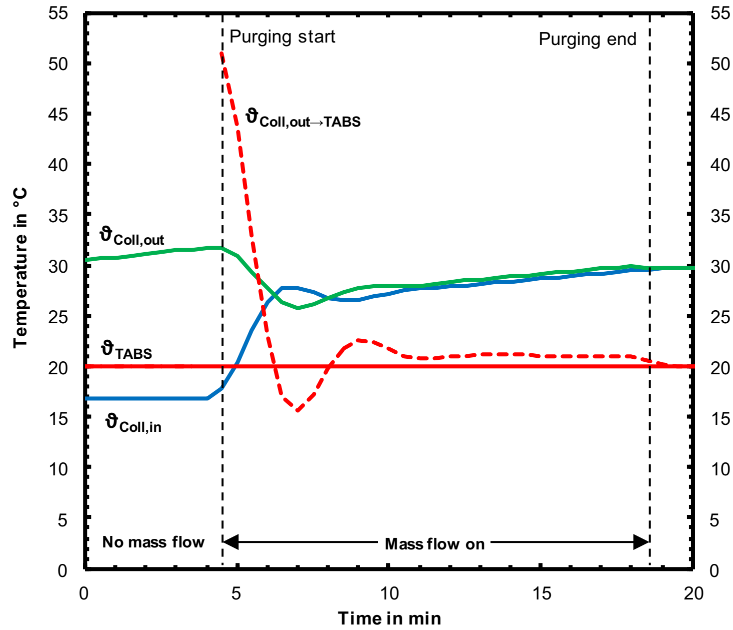

Fig. 3: Purge interval of 900 s, temperature profiles of collector in-/outlet, thermal activation and potential collector outlet temperature for TABS, Signal for purging (on/off)

At the beginning of the time period, the collector is not in operation. After purging starts, hot fluid from the outlet flows via pipes and heat exchanger to the inlet leading to a temperature increase. In contrast, the outlet temperature decreases due to colder fluid coming from the inlet and pumped through the collector field. The time lag between mass flow start and maximum/minimum temperature depends on the dead band within the collector circuit – mainly the pipes between out-/inlet and the collector field. In the example the maximum temperature at the inlet and the minimum temperature at the outlet are reached after 150 s.

After the minimum/maximum temperature, the same effect leads to rising temperatures at the outlet and decreasing temperature at the inlet. This behavior continues for 420 s at an increasing overall temperature level due to solar radiation until a constant temperature difference between inlet and outlet occurs. Before the end of purging a decreasing radiation level leads to lower outlet temperatures.

The potential collector temperatures are calculated according to Eq. 4 depending on the temperature difference between collector outlet and inlet. The diagram indicates exemplarily heat sink and potential collector temperature for the thermal activation. The demand signal is determined at the end of the purging interval. Due to the very small temperature difference after 900 s the controller determines a potential outlet temperature which is almost at the same level as the temperature of the thermal activation itself. Thus, the controller gives no demand signal and the purging is stopped (break interval of 30 min in the base case) with no collector operation.

The profile of the potential outlet temperature shows that the period length of purging may have a strong effect on the controller decision. Until 90 s the controller measures a significant temperature increase leading to a high potential collector temperature up to 50°C while a purging interval of 150 s even results in a negative collector increase and thus in potential collector temperature below its heat sink temperature. It may be concluded that the operation time and the yield of the collector strongly depends on the purging interval, which is the topic of the next Section.

4.2 Variation of purging time

Section 4.1 depicts a strong dependency between purging interval length and the resulting demand signal for one exemplary purging period. In this section, the purging interval is varied between minimum and maximum value according to Table 1 to find the effects on the annual system performance. Apart from the main energy amounts – collector yield and auxiliary energy demand (electricity) - Figure 4 shows the overall purging time and the operation time of the collector. Besides several variants of the Prac-Ctrl the figure gives the results of the Id-Ctrl.

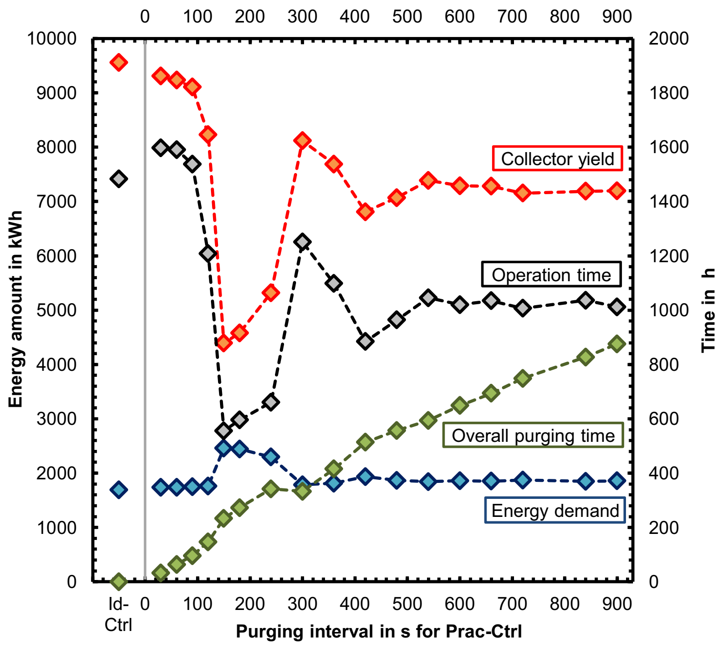

Fig. 4: Variation of purging time (break interval constant at 30 min) for the Prac-Ctrl and results for the Id-Ctrl

The purging interval affects the operation time of the collector significantly, varying between 1600 h at 30 s and 560 h at 150 s. The profile of the operation time values roughly reflects the expected behavior considering the collector temperature profile of Figure 3. The collector is switched on more frequently at a purging interval with a distinct positive temperature increase in Figure 3 compared to less operation time with smaller or even negative temperature differences between out- and inlet.

The collector yield follows the same profile as the operation time. Thus, purging intervals with frequent collector operation lead to a higher collector yield and a lower energy demand. The latter increases by more than 40% at a purging interval of 150 s compared to 1740 kWh at 30 s, which is app. 2.5% more than with the Id-Ctrl. As expected, the Id-Ctrl leads to the lowest energy demand with the highest collector yield and a slightly smaller electricity demand for the collector pump due to absence of purging.

Apart from the purging time the frequency of collector operation depends on the break between two purging intervals. Figure 5 presents annual values of time and cycles for collector operation and purging for different combinations of purging and break intervals.

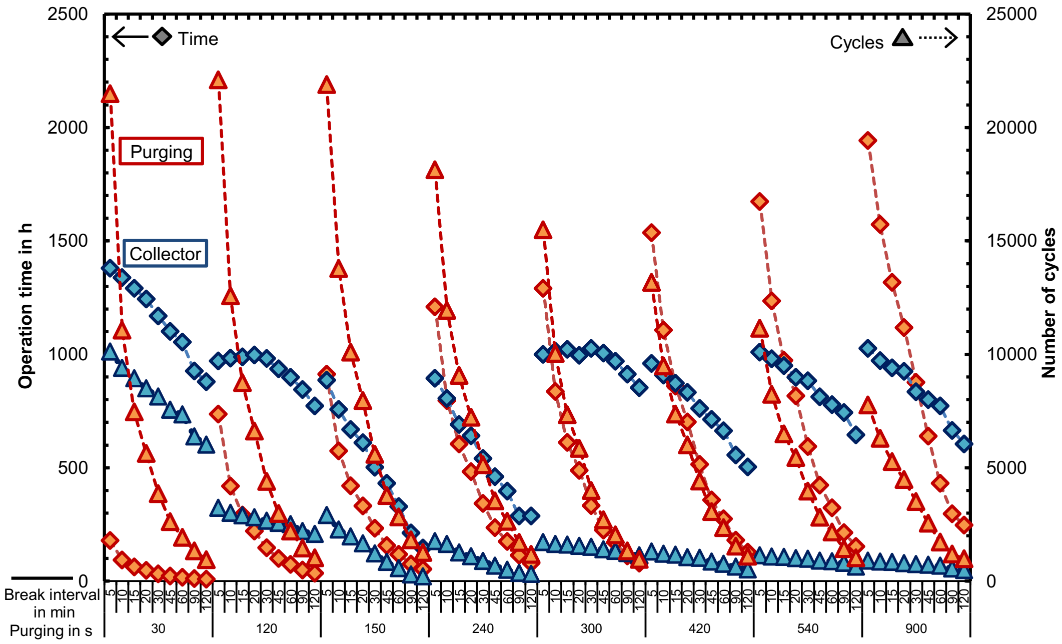

Fig. 5: Operation time and number of cycles for purging and collector operation for different purge and break intervals

The figure displays how the purging interval affects the operation time and which variant depends additionally on the break interval length. Basically, the overall purging time increases steadily with the purging interval length and the cycling frequency decreases due to less purging events above the purging duration of 150 s. However, the cycling frequency shows an increase between 30 s to 150 s, which is an indication that the collector often switches off after purging, what is leading to more purging cycles (especially at 150 s). Likewise the collector operation time gives high values at e.g. 30 s or 300 s and significantly lower values especially at 150 s. In the latter case, the break interval has a higher influence on the operation time with a significant increase at small break intervals – e.g. purging of 150 s and 5 min break interval leads to a longer operation time than 30 s purging and a break interval of 2 h.

Figure 6 shows how the different operation time values affect the collector yield and energy demand. The collector yield is divided into the fractional yield of the three different heat sinks – thermal activation, buffer storage and ground heat exchanger.

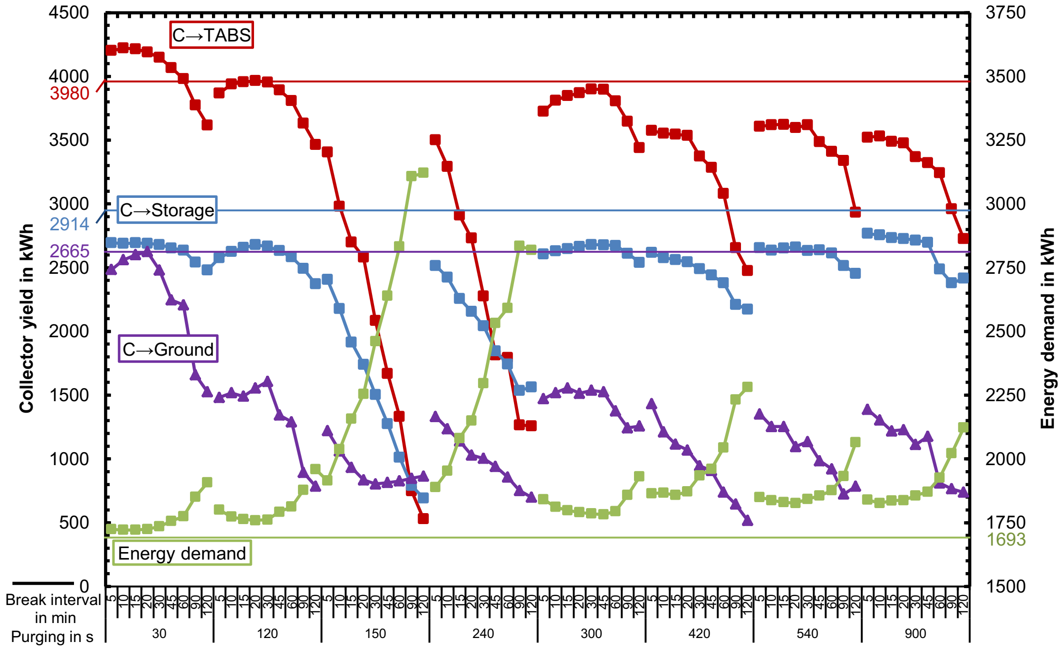

Fig. 6: Collector yield and energy demand for different purge and break intervals, the results of the Id-Ctrl are included as continuous lines with given values on the y- axis

Variants with a high collector operation time according to Figure 5 lead to high collector yields and vice versa. Especially purging intervals of 150 s or 240 s show a high dependency on the break interval. The highest collector yields are reached at a purging interval of 30 s. Here, the yield of TABS is even higher than with the Id-Ctrl while the yield of the buffer storage is lower leading to a higher overall energy demand.

Like the other heat sinks, the charging of the ground heat exchanger shows a high dependency on the purging parameters. Almost the same yield as with the Id-Ctrl is reached at a purging interval of 30 s and a 20 min break while the yield drops to 500 kWh at 420 s purging and a 120 min break. In contrast to the other collector yield values, the charging of the ground shows a higher dependency of the break interval for almost all purging intervals.

In summary, with an optimum adjustment of the purge parameters the Prac-Ctrl is able to reach almost the same collector yield and energy demand compared to the Id-Ctrl.

4.3 *Factor for potential collector output*

Both control strategies primarily determine the demand signals for all three heat sinks. If both buffer storage and TABS may be charged by the current solar potential, the ratio of the potential collector output is calculated and compared to a fixed value including a hysteresis offset, see Eq. 2. Simulations allow the evaluation of different values for the factor W_{Set} as shown in Fig. 7. In this example the Prac-Ctrl is used with the base case values for purging according to Table 1.

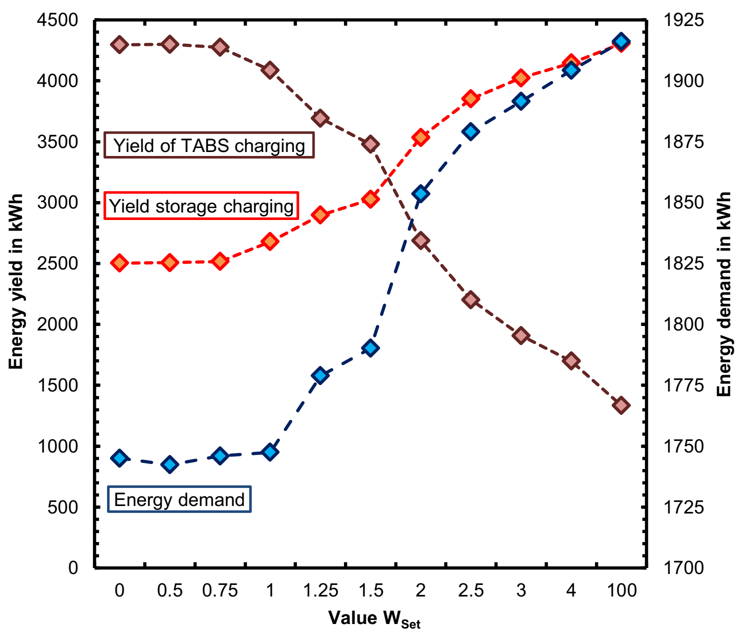

Fig. 7: Solar input to storage tank and thermal activation as well as overall energy demand for different factors W_{Set}, the factor is varied from 0 (full priority on TABS) to 100 (full priority on storage charging).

The main results are:

- The operation time and thus the solar input to the buffer storage increases with higher values of W_{Set} while the amount of the thermal activation decreases. The sum of both is not constant. The complete solar yield has a maximum value of 6807 kWh at W = 0.5 and minimum of 5641 kWh at W = 100. Thus, a priority for storage charging (W_{Set} = 100) leads to the lowest collector yield and the highest energy demand. The direct use of the solar heat via the thermal activation is advantageous compared to the charging of the buffer storage.
- There is still a considerable amount of energy delivered to the storage tank at a priority for thermal activation (W_{Set} = 0) and vice versa (W_{Set} = 100). The reason is that the controller receives a demand signal from storage and thermal activation at the same time only at 350 h/a. This is less than a sole demand signal for the buffer storage (450 h/a) or for the thermal activation (500 h/a).
- The lowest overall energy demand is reached with W_{Set} of 0.5. However, the differences from 0 to 1 (value of the base case) are less than 5 kWh.

5. Discussion

The investigation aims to demonstrate the functionality of both control concepts and to identify optimal parameters for purging and break interval of the Prac-Ctrl for one specific example.

The detailed view on the purging process in Figure 3 shows that the basic idea of the Prac-Ctrl – measuring the temperature increase in the collector field after reaching quasi-stationary conditions – is not achieved. It has been identified that the controller is not able to measure a reasonable temperature difference without considering the flow time between inlet and outlet particularly in the first minutes after the purging starts. A generalization has to take into account the hydraulic time constant of the solar loop, see Pärisch et al. (2009). The outlet temperature may be even below the inlet temperature. Due to this, small differences in the purging interval (e.g. 120 s and 150 s) may decide if the collector will be used more frequently or not and thus lead to a significant impact on the energy demand.

The temperature profile and its role in the process determining the demand signals of Figure 3 is representative for the annual performance as shown in Figure 4 and summed up in Table 2. The collector yield reaches more than 9000 kWh or less than half of it depending on the purging interval. The best results occur at short purging intervals up to 120 s. By using a small break interval, non-optimum purge intervals reach higher collector yields but are still significantly below the best variants.

Tab. 2: Summary of simulation results of Section 4, "Δϑ in Figure 3" corresponds to the difference between collector outlet and inlet temperature according to Figure 3

Purging interval	Break interval	Δϑ in Figure 3	Collector operation time	Collector yield	Energy demand
Id-Ctrl		-	1200 h	9560 kWh	1693 kWh
30 s	30 min	13.8	1170 h	9310 kWh	1735 kWh
120 s	30 min	1.4	980 h	8230 kWh	1761 kWh
150 s	30 min	-1.3	500 h	4390 kWh	2461 kWh
150 s	5 min	-	890 h	7030 kWh	1914 kWh
240 s	30 min	-0.1	540 h	5320 kWh	2296 kWh
300 s	30 min	1.2	1030 h	8120 kWh	1785 kWh
420 s	30 min	0.3	760 h	6810 kWh	1934 kWh
900 s	30 min	0.1	840 h	7200 kWh	1856 kWh

If compared with the graph in figure 3, a high potential collector outlet temperature at the moment under consideration leads to a higher collector yield and a lower energy demand.

The general problem of the Prac-Ctrl may be solved, if the outlet temperature is compared to an inlet temperature measured in advance. The time lag between both measurements corresponds to the hydraulic time constant between collectors in- and outlet and has to be defined for each system depending on the collector field size and its connection – this process has to be automized in order to be applicable in other systems.

The simulations with the shortest purging interval of 30 s indicate an energy demand value slightly above the Id-Ctrl. Therefore, it may be possible to simplify the Prac-Ctrl significantly by neglecting the purging interval. Instead, the collector is switched on, if the temperature of the (stagnating) collector is above the temperature of one heat sink using a conventional absorber temperature sensor. This modified control algorithm, which however requires a collector temperature sensor, will be analyzed in the future.

Two alternatives are presented how to react on two simultaneous demand signals – a fixed priority on one heat sink or a decision criterion based on the potential collector power. The results in Figure 7 indicate that a clear priority on the heat sink with the highest temperature level (here for the storage tank) does not lead to the lowest energy demand. Instead, the lowest energy demand occurs if the controller considers the expected thermal power with a higher priority on the thermal activation, which represents a direct use of the solar heat compared to the space heat delivery via the buffer storage.

Overall, the simulations demonstrate the functionality of both control concepts. The Prac-Ctrl leads to slightly higher energy demands than the more cost intensive Id-Ctrl, but the difference is below 2% including the energy consumption for the pumps. Therefore, the Prac-Ctrl represents a reasonable approach for real systems. It is expected that a change in the control algorithm as stated above will increase its reliability and performance. The final version of the controller will be implemented in a test building of the system introduced in Section 3 to investigate the control behavior under real conditions.

6. Acknowledgement

The project SH-T-opt (FKZ 0325962A) is funded by the German Federal Ministry for Economic Affairs and Energy based on a decision of the German Federal Parliament. Project partners of the ISFH are the HELMA Eigenheimbau AG situated in Lehrte and RESOL – Elektronische Regelungen GmbH situated in Hattingen. The authors are grateful for the financial support. The content of this paper is in the responsibility of the authors.

7. References

Kalogirou, SA, 2009. Solar energy engineering: processes and systems, Academic Press.

Klein SA, Beckmann WA, Mitchell JW, Duffie JA, Freeman TA, 2009. TRNSYS 17, A Transient System Simulation Program, Solar Energy Laboratory University of Wisconsin, Madison

Pärisch, P, Filler, G, Tepe R, 2009. Innovativer Regler für Thermische Solaranlagen (in German), Final Report, Deutsche Bundesstiftung Umwelt

Glembin J, et al., 2014. Solar active building with directly heated concrete floor slabs, Energy Procedia 48, pp. 561-570.